

Selective Functionalization of Gold Microstructures with Ferrocenyl Derivatives via Reaction with Thiols or Disulfides: Characterization by Electrochemistry and Auger Electron Spectroscopy

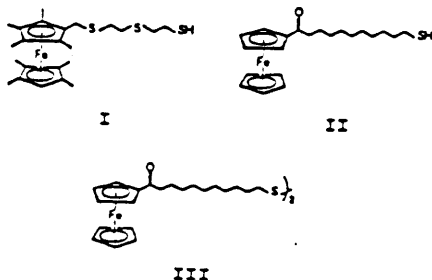
James J. Hickman,[†] David Ofer,[†] Chaofeng Zou,[†] Mark S. Wrighton,^{*,†} Paul E. Laibinis,[†] and George M. Whitesides^{*,†}

Contribution from the Department of Chemistry, Massachusetts Institute of Technology, Cambridge, Massachusetts 02139, and the Department of Chemistry, Harvard University, Cambridge, Massachusetts 02138. Received August 13, 1990

Abstract: Auger electron spectroscopy and electrochemistry show that ferrocenyl thiols or disulfides can be used to modify selectively the Au microelectrodes ($\sim 2 \mu\text{m} \times 90 \mu\text{m} \times 0.1 \mu\text{m}$) on a Si_3N_4 substrate. The Auger technique shows the selectivity of chemisorption of thiol ($-\text{SH}$) or disulfide ($-\text{SS}-$) groups on Au relative to their physisorption on Si_3N_4 to be at least 100:1. Immersion of Au electrodes into solutions containing (1-mercapto-3,6-dithiaheptanyl)octamethylferrocene (I), 11-mercapto-undecanoylferrocene (II), or bis[10-(ferrocenylcarbonyl)decyl] disulfide (III) yields modified Au electrodes showing about one monolayer of a reversibly redox active ferrocene reagent. Compound I yields an $E_{1/2}$ about 550 mV more negative than that for II or III (which both have the same $E_{1/2}$ values). The electroactive layer from I on Au is far more labile than that from II or III. Loss of I takes place with a $t_{1/2}$ of ~ 2 h at 298 K in a hexane solution; little or no loss of electroactive material derived from II or III occurs on the same time scale. When Au electrodes modified with I are immersed in hexane solutions of II, replacement of I by II occurs cleanly and at a rate that is the same as loss of I in hexane only. Detailed procedures for Auger element mapping of organic monolayers at high lateral resolution ($\sim 0.1 \mu\text{m}$) are presented, and such maps give a reliable image of the distribution of molecules on the surface.

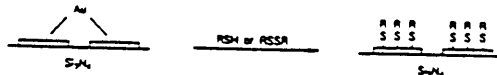
We report the selective derivatization of Au microelectrode arrays using redox active molecules that have thiol or disulfide functional groups. The resulting microstructures have been characterized by Auger electron spectroscopy (AES) and cyclic voltammetry. This paper includes the details of our methodology for high lateral resolution AES imaging of monolayer-derivatized microstructures. We have previously reported such results without fully detailing the procedures employed.^{1,2}

The formation and structure of molecular monolayers on Au derived from alkane thiols and disulfides have been extensively studied on macrostructures,³⁻¹² including a recent report of attachment of electroactive groups to Au via reaction with thiol groups.¹³ Our work focuses on the selective derivatization of Au on an insulating Si_3N_4 substrate (Scheme I). Previously, we have shown such selective chemistry for alkanethiols¹ and have shown that redox active isonitriles can be bound to Pt microstructures.² Our aim is to combine microfabrication and coordination chemistry to rationally functionalize surfaces. Here we show the selective functionalization of Au on Si_3N_4 with molecules I-III.



This selective adsorption allows derivatization of Au with redox reagents having different redox potentials. Molecules I-III all selectively functionalize the Au, but the resulting structures from II or III are far more rugged than the structure from I. Use of I allows investigation of its replacement from a surface, owing

Scheme I. Selective Functionalization of Au Microelectrodes



to its relative lability and its more negative $E_{1/2}$ value compared to the $E_{1/2}$ for reagents II and III.

Experimental Section

Chemicals. The $[\text{m-Bu}_4\text{N}]\text{PF}_6$ was obtained from Aldrich and recrystallized from EtOH. CH_3CN was obtained from Omnisolv and distilled from CaH_2 .

(1-Mercapto-3,6-dithiaheptanyl)octamethylferrocene (I) was synthesized according to literature procedures.¹⁴

11-(Thioacetyl)undecanoylferrocene. 11-Bromoundecanoyl ferrocene¹⁵ (6.53 g, 15 mmol) was combined with NaOMe (1.08 g, 20 mmol) and thioacetic acid (2.06 g, 27 mmol) in 60 mL of MeOH and refluxed for 18 h. The mixture was concentrated and purified by chromatography (silica, 3% acetone/hexanes) to yield the desired product as a reddish

- (1) Laibinis, P. E.; Hickman, J. J.; Wrighton, M. S.; Whitesides, G. M. *Science (Washington, D.C.)* 1989, 245, 845-847.
- (2) Hickman, J. J.; Zou, C.; Ofer, D.; Harvey, P. D.; Wrighton, M. S.; Laibinis, P. E.; Bain, C. D.; Whitesides, G. M. *J. Am. Chem. Soc.* 1989, 111, 7271-7272.
- (3) Nuzzo, R. G.; Allara, D. L. *J. Am. Chem. Soc.* 1983, 105, 4481-4483.
- (4) Nuzzo, R. G.; Fusco, F. A.; Allara, D. L. *J. Am. Chem. Soc.* 1987, 109, 2358-2368.
- (5) Bain, C. D.; Troughton, E. B.; Tao, Y.-T.; Evall, J.; Whitesides, G. M.; Nuzzo, R. G. *J. Am. Chem. Soc.* 1989, 111, 321-335.
- (6) Diem, T.; Czajka, B.; Weber, B.; Regen, S. L. *J. Am. Chem. Soc.* 1986, 108, 6094-6095.
- (7) Bain, C. D.; Biebuyck, H. A.; Whitesides, G. M. *Langmuir* 1989, 5, 723-727.
- (8) Porter, M. D.; Bright, T. B.; Allara, D. L.; Chidsey, C. E. D. *J. Am. Chem. Soc.* 1987, 109, 3559-3568.
- (9) Strong, L.; Whitesides, G. M. *Langmuir* 1988, 4, 546-558. Chidsey and Loiacono¹¹ have recently reanalyzed the data of Strong and Whitesides and established that the lattice of the alkane thiolate monolayer is rotated by 30° with respect to the (111)Au lattice.
- (10) Bain, C. D.; Whitesides, G. M. *J. Phys. Chem.* 1989, 93, 1670-1673.
- (11) Chidsey, C. E. D.; Loiacono, D. N. *Langmuir* 1990, 6, 682-691.
- (12) Nuzzo, R. G.; Dubois, L. H.; Allara, D. L. *J. Am. Chem. Soc.* 1990, 112, 558-569.
- (13) Chidsey, C. E. D.; Bertozzi, C. R.; Putviniski, T. M.; Mujser, A. M. *J. Am. Chem. Soc.* 1990, 112, 4301-4306.
- (14) Zou, C.; Wrighton, M. S. *J. Am. Chem. Soc.* 1990, 112, 7578-7584.
- (15) Okahata, Y.; Enna, G.; Takenouchi, K. *J. Chem. Soc., Perkin Trans.* 2 1989, 835-843.

* Address correspondence to these authors.

[†] Massachusetts Institute of Technology.

[†] Harvard University.

orange solid (5.50 g, 12.8 mmol, 85% yield); mp 55–56 °C; $^1\text{H NMR}$ (CDCl_3) δ 4.76 (t, $J = 2$ Hz, 2 H), 4.47 (t, $J = 2$ Hz, 2 H), 4.17 (s, 5 H), 2.84 (t, $J = 7$ Hz, 2 H), 2.67 (t, $J = 7$ Hz, 2 H), 2.30 (s, 3 H), 1.65 (m, 2 H), 1.6 (m, 2 H), 1.3–1.4 (m, 12 H). Anal. Calcd (found) for $\text{C}_{27}\text{H}_{32}\text{FeO}_2\text{S}$: C, 64.48 (64.50); H, 7.53 (7.61); Fe, 13.04 (12.50); S, 7.48 (7.89).

11-Mercaptoundecanoylferrocene (II). 11-(Thioacetyl)undecanoylferrocene (5.04 g, 11.8 mmol) was combined with 50 mL of degassed absolute EtOH and 5 mL of concentrated HCl and refluxed for 2 h. The solution was concentrated, and II was obtained by chromatography (silica, 5% acetone/hexanes) in 61% yield (2.76 g, 7.1 mmol); mp 57–58 °C; $^1\text{H NMR}$ (CDCl_3) δ 4.76 (t, $J = 2$ Hz, 2 H), 4.47 (t, $J = 2$ Hz, 2 H), 4.17 (s, 5 H), 2.67 (t, $J = 7$ Hz, 2 H), 2.50 (q, $J = 7$ Hz, 2 H), 1.65 (m, 2 H), 1.6 (m, 2 H), 1.31 (t, $J = 7$ Hz, 1 H), 1.3–1.4 (m, 12 H). Anal. Calcd (found) for $\text{C}_{27}\text{H}_{30}\text{FeOS}$: C, 65.28 (65.38); H, 7.83 (7.62); Fe, 14.45 (14.16); S, 8.30 (8.39).

Bis[10-(ferrocenylcarboxyl)decyl] disulfide (III). 11-Mercaptoundecanoylferrocene (0.56 g, 1.45 mmol) was dissolved in absolute EtOH and titrated with an EtOH/ I_2 solution until a brown color persisted. The solution was concentrated, and III was obtained by chromatography (silica, 2% acetone/hexanes) followed by 5% acetone/hexanes) in 75% yield (0.42 g, 0.54 mmol); mp 64–65 °C; $^1\text{H NMR}$ (CDCl_3) δ 4.76 (t, $J = 2$ Hz, 4 H), 4.47 (t, $J = 2$ Hz, 4 H), 4.17 (s, 10 H), 2.67 (t, $J = 7$ Hz, 4 H), 2.66 (t, $J = 7$ Hz, 4 H), 1.65 (m, 8 H), 1.3–1.4 (m, 24 H). Anal. Calcd (found) for $\text{C}_{42}\text{H}_{52}\text{Fe}_2\text{O}_4\text{S}_2$: C, 65.45 (64.91); H, 7.59 (7.43).

Electrodes and Surface Modification. The microelectrode experiments were carried out on arrays of eight individually addressable parallel Au microelectrodes (~ 2 μm wide, ~ 90 μm long, ~ 0.1 μm thick) separated from each other by ~ 1.4 μm on a flat Si_3N_4 -coated Si substrate.¹⁶ The leads connecting the microelectrodes to macroscopic bonding pads were encapsulated beneath an additional layer of Si_3N_4 . Macroelectrodes consisted of 2000 Å of Au (99.999%) evaporated onto 100-mm diameter Si wafers coated with a 100-Å adhesion layer of Cr. The Au-coated wafers were cut into approximately 1 cm \times 4 cm pieces. Contact for electrochemical experiments was made by using alligator clips. Both the macroelectrodes and microelectrode arrays were cleaned by first sonicating for ~ 10 min in each of the three solvents in the order of increasing polarity (hexane, acetone, and CH_3OH). The sonication was followed by a plasma treatment in a Harrick PDC-23G plasma cleaner; the electrodes were treated for 3 min in a flowing O_2 plasma, 0.3 Torr at medium power (40 W), and 1 min in a flowing H_2 plasma, 0.5 Torr at low power (30 W). The pretreatment procedure used to clean the Au results in reproducible derivatization with I–III for macroelectrodes. For microelectrodes, however, less reproducibility is found, owing to difficulties in removing residual photoresist from the microfabrication process. Immediately upon removal from the plasma cleaner, electrodes were immersed in a deoxygenated 1 mM solution of I, II, or III in the appropriate solvent [hexane for I, tetrahydrofuran (THF) for II, and 20:1 hexane/EtOH for III] for approximately 24 h. After derivatization, the electrodes were rinsed with CH_3CN and characterized by electrochemical methods and surface spectroscopy.

Electrochemical Methods. Electrochemical measurements were carried out with a Pine Instruments Model RDE-4 bipotentiostat. Voltammetric traces were recorded by using a Kipp and Zonen Model BD 91 XY recorder. Linear sweep cyclic voltammetry was performed in $\text{CH}_3\text{CN}/0.1$ M $[\text{n-Bu}_4\text{N}]\text{PF}_6$ at 258 or 298 K in Ar-purged solutions. Pt gauze was used as a counter electrode and oxidized Ag wire as a quasi-reference. The electrodes were then rinsed with CH_3CN and placed in the appropriate deoxygenated solution or prepared for surface analysis.

Auger Electron Spectroscopy. Auger electron spectroscopy (AES) was done by using a PHI 660 scanning Auger microprobe. Samples were grounded to copper tape with Ag point, and the tape was affixed to the spectrometer stage with metal screws. Obtaining Auger electron spectral data for molecular monolayers, particularly element maps at high lateral resolution (~ 0.1 μm), proved to be difficult. Conditions necessary to analyze molecular monolayers by AES at high lateral resolution are presented in the results section (vide infra).

Results and Discussion

a. Electrochemical Behavior of Au Macro- and Microelectrodes Modified by Reaction with I–III. Reaction of I, II, or III with Au surfaces results in the persistent attachment of reversibly redox active molecules. The presence of redox active molecules can be established by linear sweep cyclic voltammetry in $\text{CH}_3\text{CN}/0.1$

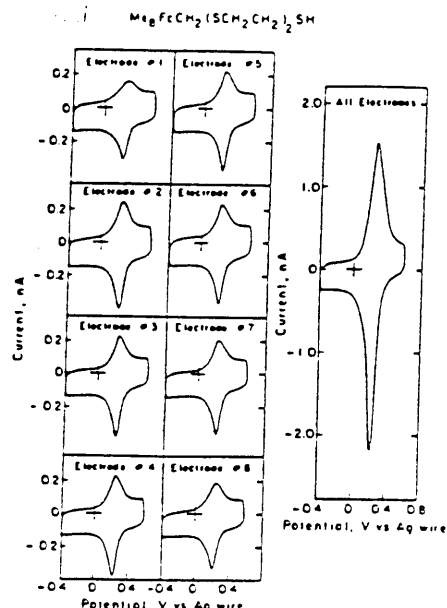


Figure 1. Cyclic voltammetry (500 mV/s; in $\text{CH}_3\text{CN}/0.1$ M $[\text{n-Bu}_4\text{N}]\text{PF}_6$ at 258 K) of eight Au microelectrodes derivatized with a 1 mM solution of I in hexane for 24 h.

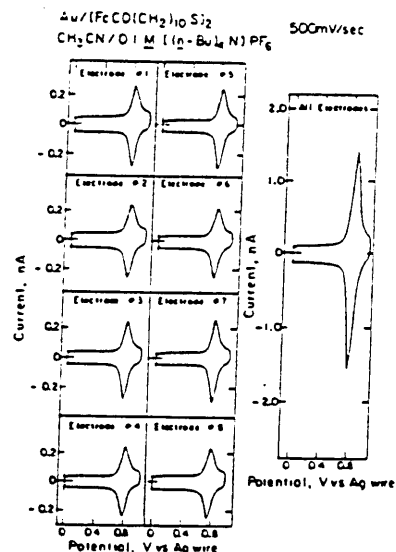


Figure 2. Cyclic voltammetry of eight Au microelectrodes derivatized with a 1 mM solution of III in 20:1 hexane/EtOH for 48 h.

M $[\text{n-Bu}_4\text{N}]\text{PF}_6$. Figures 1 and 2 show data for Au microelectrode arrays modified by reaction with I and III, respectively. Modification of Au microelectrodes with II gives a response indistinguishable from that found for III with respect to coverage and $E_{1/2}$ for the surface-confined redox molecule. Qualitative studies show, however, that II reacts more rapidly than III, consistent with earlier studies concerning the relative reactivity of thiols and disulfides toward Au.¹⁷ Electrochemical behavior of Au macroelectrodes is the same as that for Au microelectrodes and

(16) Kittlesen, G. P.; White, H. S.; Wrighton, M. S. *J. Am. Chem. Soc.* 1984, 106, 7319–7396.

(17) Bain, C. D.; Whitesides, G. M. *Langmuir* 1989, 5, 723–727.

1130 *J. Am. Chem. Soc.*, Vol. 113, No. 4, 1991

consistent with reversible electrochemistry found for $\text{Fc}(\text{CH}_2)_8\text{SH}$ or $\text{FcCO}_2(\text{CH}_2)_{11}\text{SH}$ (Fc = ferrocenyl) bonded to Au macroelectrodes.¹³ The electrochemical response in Figures 1 and 2 shows a somewhat larger charging current than might be expected. The larger charging current is attributed to capacitance associated with the Si_3N_4 encapsulating layer over the leads used to address the microelectrodes.

Part of the significance of the data in Figures 1 and 2 is the demonstration of the electrode-to-electrode reproducibility of coverage of electroactive material. Each of the eight individually addressable microelectrodes shows nearly the same amount of electroactive material for a given derivatizing reagent, based on the integral of the current-potential curve corresponding to the Faradaic current for oxidation and reduction of the ferrocene centers. In Figure 1 the eight microelectrodes derivatized with I show an average coverage of $(3.1 \pm 0.3) \times 10^{-10}$ mol/cm², whereas the data for III in Figure 2 show somewhat larger average coverage of $(4.6 \pm 0.2) \times 10^{-10}$ mol/cm². The electrode-to-electrode variation is modest, but it should be emphasized that the pretreatment of microelectrode arrays does not always successfully remove residual photoresist from the microfabrication. Superior reproducibility is found for Au macroelectrodes, compared to microelectrodes, with respect to consistency of coverage of redox active material. The larger coverage of redox material from II or III compared to that from I is a general finding and is expected on the basis of steric considerations. However, the layer on Au from the long-chain molecules II or III might dissolve some additional II or III, thereby giving some additional electroactive material not bound by a Au-S interaction.¹⁴ Such behavior is less likely for molecular layers from I, owing to the short chain. The absolute coverage of a close-packed monolayer of long-chain alkyl thiol on (111)Au crystals is estimated to be 7.7×10^{-10} mol/cm².⁹ Other workers have found that ferrocenyl alkyl thiols give a monolayer coverage of $\sim 4.5 \times 10^{-10}$ mol/cm²,¹² in close accord with our data for surfaces derivatized with II or III.

The cyclic voltammetry of Au electrodes derivatized with I, II, or III in $\text{CH}_3\text{CN}/0.1 \text{ M } [n\text{-Bu}_4\text{N}]\text{PF}_6$ at 298 K shows persistent attachment of the ferrocenyl-based reagents. Repetitive cycling between the reduced and oxidized forms of the molecules results in little or no loss of electroactive material on the time scale of 1 h, but long-term changes do occur (vide infra). The durability of electrodes modified with I, II, or III is sufficiently great that routine electrochemical characterization is possible. The $E_{1/2}$ values, taken to be the average position of the anodic and cathodic waves, are +0.2, +0.8, and +0.8 V vs Ag quasi-reference for surface-confined ferrocenyl centers derived from I, II, and III, respectively. The more negative value of $E_{1/2}$ for I is consistent with the presence of the eight electron-releasing Me groups on the cyclopentadienyl rings. For electrodes modified with I, the anodic and cathodic peaks have different shapes (Figure 1), consistent with changes in the structure of the electroactive monolayer film upon oxidation. In contrast, the cyclic voltammetry waves for II and III are more symmetrical, consistent with smaller changes in monolayer film structure upon oxidation. The differences between electrodes modified with I vs II or III could be due to the importance of chain-chain interactions in maintaining a constant monolayer film structure. The peak-to-peak separation in the cyclic voltammograms at 500 mV/s is <60 mV and close to 0 mV at 100 mV/s. The peak currents are proportional to sweep rate up to at least 1 V/s, in accord with fast electron transfer from the bound molecules to the electrodes. Though detailed comparisons have not been made, the cyclic voltammetry response in aqueous electrolyte (pH 0-10) of Au electrodes modified with II or III is qualitatively the same (shape and position) as that in $\text{CH}_3\text{CN}/0.1 \text{ M } [n\text{-Bu}_4\text{N}]\text{PF}_6$. We conclude that reagents I-III all represent viable reagents for the functionalization of Au electrodes with well-behaved, ferrocene-based redox systems.

(18) Bunding Lee, K. A.; Mowry, R.; McLennan, G.; Finkles, H. O. *J. Electroanal. Chem.* 1988, 246, 217-224.

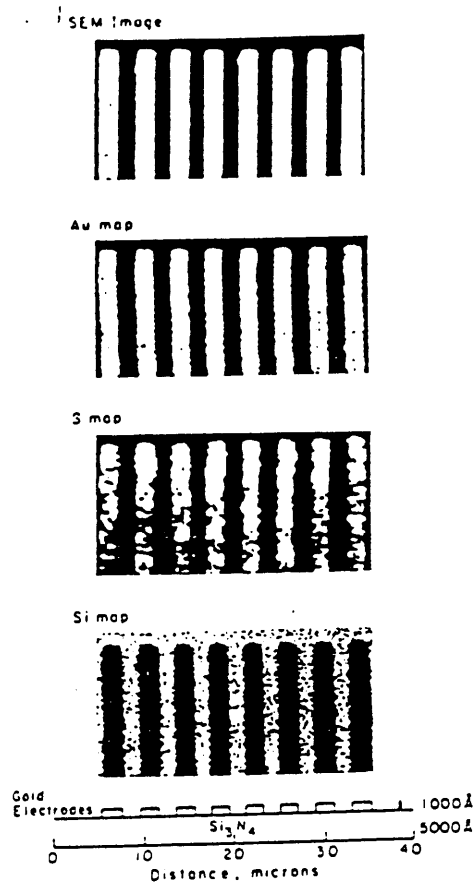


Figure 3. Scanning electron micrograph (SEM) and scanning Auger element maps of Au, S, and Si for a Au microelectrode array derivatized with I. The device is the same one characterized by the cyclic voltammetry in Figure 1.

b. Proof of Selective Binding of I-III to Au vs Si_3N_4 : Auger Electron Spectroscopy. Auger electron spectroscopy (AES) has proven to be a useful technique for characterization of electrodes modified with molecular materials.¹⁹ We have used AES to establish that molecules I-III bind selectively to the Au microelectrodes and not to the Si_3N_4 substrate, as shown in Scheme 1. This result is expected, on the basis of our earlier demonstration of such selective binding of simple alkanethiols on Au vs Si_3N_4 .¹ From quantitative AES studies on the Au and Si_3N_4 after derivatization with I, II, or III we find that the selectivity for the Au is at least 100 to 1.

One particularly compelling analytical method is to record the relative concentration of sulfur over the surface of the microelectrode array. So-called Auger element maps reveal the location of surface-confined molecules relative to the Au microstructures. Figure 3 shows a map for S, Si, and Au along with a scanning electron micrograph of a Au microelectrode array derivatized with I. The brighter regions in a given map correspond to higher concentrations of the element assayed. The important conclusion is that the S shows high concentration in the same region where Au is detected and S is not detectable in the region where Si (from Si_3N_4) is detected. We thus conclude that I reacts selectively with Au surfaces and not with the Si_3N_4 .

(19) (a) Hubbard, A. T. *Chem. Rev.* 1988, 88, 633-656. (b) Bruce, J. A.; Wrighton, M. S. *J. Am. Chem. Soc.* 1982, 104, 74-82. (c) Bruce, J. A.; Wrighton, M. S. *J. Electroanal. Chem.* 1981, 122, 93-102.

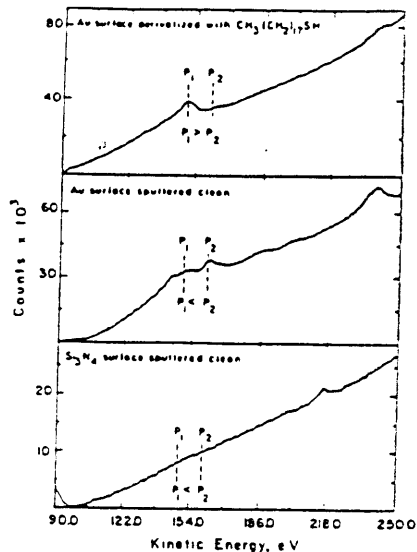


Figure 4. Auger scans (90–250 eV) of a Au microelectrode surface derivatized with $\text{CH}_3(\text{CH}_2)_{17}\text{SH}$ (top), clean Au (middle), and a clean Si_3N_4 surface (bottom). Note different vertical scales for the Au and Si_3N_4 . P_1 and P_2 are the points used in mapping S (cf. Figure 3 and text).

Auger element mapping at high lateral resolution for organic monolayers is difficult, owing to low signal, to e^- beam-induced degradation from high beam current densities and high voltages, and to drift of the instrument during the time (~ 2 – 4 h) required to map a $\sim 30 \times 30 \mu\text{m}$ region at $\sim 0.1\text{-}\mu\text{m}$ resolution. The surface spectroscopy is also complicated by surface charging of the insulating substrate. Surface charging is a problem common in Auger electron microscopy, and we have minimized this problem by tilting the sample such that the e^- beam makes an angle of 40 – 60° with the plane of the surface.²⁰ Sample degradation has been minimized by use of low beam currents (0.1 – 5 nA) with beam voltages of 8 – 10 kV. Low beam voltages minimize damage, but the higher values help to overcome surface charging. Although exact parameters used vary somewhat from sample to sample, at high lateral resolution the beam diameter is always ~ 100 nm. This diameter results in a large beam current density: ~ 1 – 65 A/cm². The actual dose to a given sample area obviously depends on the time to acquire an adequate signal-to-noise ratio. To obtain our element maps, the $\sim 30 \times 30 \mu\text{m}$ region to be investigated was typically scanned in a line-by-line fashion taking 170 equally spaced data points per line. Generally, 170 lines were scanned, giving a total of 28 900 pixels in the map. The time to obtain good signal-to-noise maps for elements unique to the organic monolayer (e.g., S) varied, but typically recording the entire map required 2–4 h. Thus, the residence time for each pixel of the map is 0.25–0.5 s. The conditions used thus mean that each pixel of the map could have received a dose of as much as 2×10^{14} mol of electrons, while each pixel would have at most $\sim 8 \times 10^{-20}$ mol of a molecular monolayer from I, II, or III. Clearly, equivalent Auger signal-to-noise ratios for routine analysis of molecular monolayers on macroscopic surfaces will involve qualitatively less dose per molecule than needed for our high lateral resolution mapping. The viability of our methodology has been established by demonstration of sample-to-sample repeatability.

Mapping S on Au is further complicated by the overlap of a Au peak with the strongest peak for S. Figure 4 shows the Auger spectra of the Si_3N_4 and Au regions of an array derivatized with I and includes the spectrum for the Au after it was cleaned with

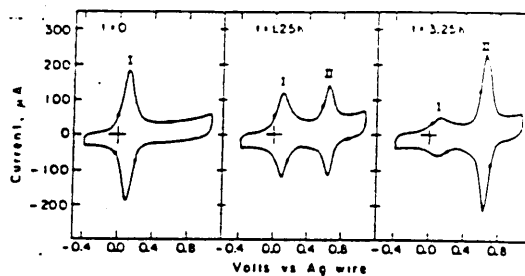


Figure 5. Cyclic voltammetry ($\text{CH}_3\text{CN}/0.1$ M $[\text{n-Bu}_4\text{N}]\text{ClO}_4$; 500 mV/s) of a Au electrode derivatized with I (left) and then exposed to a 1 mM solution of II in hexane for 1.25 h (middle) and the same electrode after 3.25 h in a hexane solution of II (right). At 19 h, II has completely replaced I on the surface.

an Ar ion beam to remove the S-containing molecule. The procedure used in mapping S is to first record the counts at the energy corresponding to the S peak, P_1 in Figure 4, for each pixel of a line. The counts on the high-energy side of the S peak at an energy chosen to correspond to a maximum in the Au spectrum, P_2 in Figure 4, are then recorded for each pixel of the line. P_1 and P_2 in the spectrum for clean Au correspond to maxima for the interfering Au peaks. P_1 for clean Au is always lower than P_2 . It is important to note that the comparison of P_2 and P_1 is made after baseline correction. Accordingly, when $P_1 > P_2$, we conclude S to be present for a given pixel, and the brightness in the map is proportional to P_1/P_2 . The Si_3N_4 surface has no interfering Auger signals, and detection (or lack) of S is unambiguous. The important point is that by selecting P_2 to be at the maximum of a Au peak that is larger than the interfering Au peak at P_1 , we can unambiguously detect S on Au by concluding S to be present to the extent P_1 exceeds P_2 . If anything, our procedures underestimate the amount of S on Au. Thus, the element maps shown in Figure 3, and those acquired earlier¹ for alkanethiols on Au/ Si_3N_4 , are reliable images of the distribution of S-containing molecules over the surface.

It is significant that our Auger mapping technique represents a way to obtain elemental composition of a molecular monolayer on a surface at very high lateral resolution ($\sim 0.1 \mu\text{m}$). In principle, secondary ion mass spectrometry (SIMS) could yield similar resolution, but such experiments have not yet been reported. X-ray photoelectron spectroscopy (XPS) could likewise be workable, in principle, but techniques to focus an X-ray beam to small spot sizes are still being developed. Scanning Raman microscopy and FTIR microscopy, important tools for establishing molecular structure on surfaces, are limited in lateral resolution by the wavelength of light. Thus, the Auger mapping technique stands as an important method for determining surface distribution of molecular reagents.

c. Reactivity of Surfaces Functionalized with I or II. As noted above, Au electrodes functionalized with I, II, or III yield durable, reversible redox systems. The durability of electrodes derivatized with I was, however, much less than that of electrodes derivatized with II or III. We have carried out some preliminary studies of exchange chemistry with I and II to begin to establish factors controlling rates and equilibrium positions in such systems.

One significant set of results is summarized by the data in Figures 5 and 6. Figure 5 shows the behavior of a Au electrode first modified with I and then exposed to 1 mM II in hexane at 298 K. The cyclic voltammetry indicates loss of the response attributed to I and growth of a signal for II. Importantly, the rate of loss ($t_{1/2} \sim 2$ h) of I is the same for an electrode exposed to hexane only (Figure 6). For the electrode first exposed to I and then exposed to II, the response is ultimately only that of II, showing the same coverage that would be found for an electrode derivatized initially with only II. Derivatization of a Au electrode with a 1:1 hexane solution of I and II yields an electrochemical response showing mainly ($>95\%$) II, even at short (~ 1 h) derivatization times. For Au initially derivatized with II and then

(20) Briggs, D.; Seah, M. P. *Practical Surface Analysis by Auger and X-ray Photoelectron Spectroscopy*; Wiley: New York, 1983; pp 234–235.

1132

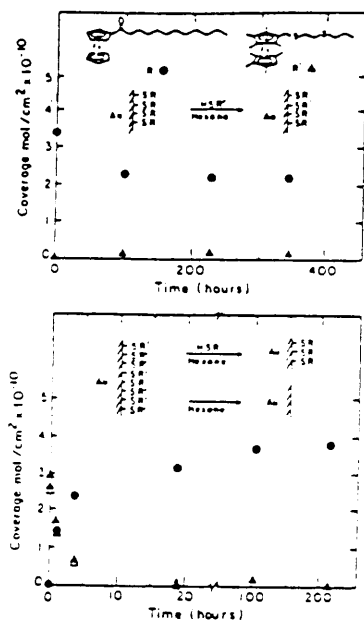


Figure 6. Time dependence of the surface coverage of I (●) and II (▲) for a Au macroelectrode initially derivitized with II and placed in a hexane/1 mM I solution (top) and for a Au macroelectrode initially derivitized with I and exposed to hexane/1 mM II (bottom). The bottom panel also includes data for an independent experiment showing coverage of I on Au upon exposure to hexane only (Δ). All coverages were measured by cyclic voltammetry in $\text{CH}_3\text{CN}/0.1 \text{ M } [n\text{-Bu}_4\text{N}]\text{PF}_6$ at 500 mV/s.

soaked in hexane only, we find some initial loss of coverage, $\sim 4.5 \times 10^{-10}$ to $\sim 3 \times 10^{-10}$ mol/cm², but even after 1300 h, additional loss of redox active material does not occur. Similarly, if an electrode is first derivitized with II and then exposed to 1 mM I in hexane, there is some initial loss of II and a small uptake of I, but thereafter virtually no changes take place over a period of at least 400 h (Figure 6).

The experiments summarized by Figure 5 and 6 show the surfaces derivitized with I to be labile, with a rate of loss of I unaffected by the presence of II in hexane. That Au surfaces derivitized with I are most labile than those derivitized with II (or III) is certain.

Conclusion

Ferrocenyl thiols and disulfides can be used to modify selectively the Au microstructures on a Si_3N_4 surface. Simple immersion of a pretreated Au microelectrode array into a solution of I, II, or III yields Au electrodes functionalized with about one monolayer of the ferrocene reagent; no molecular material is detectable on the Si_3N_4 . Auger element mapping can be used to obtain the high lateral resolution necessary to characterize microfabricated structures modified with a molecular monolayer. The octamethylferrocenyl system (I) shows a relatively negative $E_{1/2}$ value consistent with the electron-releasing nature of the CH_3 substituents. With respect to persistence of electrochemical response, all experiments show II or III to yield more durable modified Au surfaces than I. The large size of the "head group" of I and the short tether to the Au are likely factors limiting the durability of Au modified with I, in comparison to Au modified with II or III.

We can draw one mechanistic conclusion regarding the surfaces modified with I: the replacement of I by II appears to proceed by a mechanism involving loss of I followed by uptake of II, a process analogous to an $\text{S}_{\text{N}}1$ substitution mechanism for discrete coordination complexes. This conclusion is based on the observation that the rate of loss of I is unaffected by the presence of II. We caution against generalization of this simple mechanistic hypothesis, because the loss of II, for example, from the surface (Figure 6) appears to be quite different: some material is weakly bound, while the majority is firmly bound. Additional work is needed to establish factors governing rates, mechanisms, and thermodynamics for the coordination and exchange processes of thiols in solution and thiolates on Au surfaces.

Acknowledgment. M.S.W. thanks the U.S. Department of Energy, Office of Basic Energy Sciences, Division of Chemical Sciences, for support of this research. G.M.W. thanks the Office of Naval Research and the Defense Advanced Projects Agency for partial support of this research. We acknowledge use of XPS and Auger facilities acquired through the joint Harvard/MIT University Research Initiative funded by the Defense Advanced Research Projects Agency.